Magnetic field analysis using the improved global particle swarm optimization algorithm to estimate the depth and approximate shape of the buried mass

Mahdieh HEIDARI [ID], Mirsattar MESHINCHI ASL* [ID], Mahmoud MEHRAMUZ [ID], Reza HEIDARI [ID]

Department of Earth Sciences, Science and Research Branch, Islamic Azad University, Tehran, Iran

Abstract: In this paper, the optimization algorithm based on the population as improved global particle swarm optimization is described and used for inverse modelling of two-dimensional magnetic field data. This algorithm is able to estimate the parameters of depth, shape factor, amplitude coefficient, magnetic inclination angle and origin point coordinates. To evaluate the efficiency of this method, the magnetic field of an artificial model was analysed, with and without added random noise. The results suggest that the proposed algorithm is capable of model parameter estimation with high accuracy. Accordingly, the improved global particle swarm optimization algorithm was used to analyse the magnetic field of the study area in the Ileh region in Iran located in Taybad city. The study area is very rich in terms of iron resources. The estimate for the study area is that the depth of the buried mass centre is about 114.9 m and its approximate shape is similar to a horizontal cylinder based on the calculated shape factor value which is 1.76. The calculated depth is an acceptable match with the average depth of drillings.

Key words: Ileh, improved global particle swarm optimization, magnetic field

1. Introduction

Potential field methods have various applications in geophysical prospecting (*Biwas and Rao, 2021; Essa et al., 2021; Gan et al., 2022; Gokula and Sastry, 2022; Mehanee, 2022a*). One of the important goals of the interpretation of magnetic data is to determine the characteristics such as size, shape and position of the different types of underground structures for various purposes such as exploration, mining and geological studies. The subsurface

---

*corresponding author, e-mail: m.meshinchi@srbiau.ac.ir, phone: 09122902039

geological structures can be modelled into simple geometric shapes such as spheres, cylinders, or plane structures acceptably by using magnetic data (*Mehanee, et al 2021*). Parameters that control the shape and position of the geometric model such as depth, length, and radius are calculated and the parameters that produce the best magnetic field for a model are considered as the best model.

Interpretation of magnetic anomaly is remarkably important in the exploration areas according to the subsurface targets (*Nabighian et al., 2005; Abdelrahman et al., 2009; Ekinci et al., 2014*). Also, the magnetic method can be used in hydrocarbon exploration (*Abubakar et al., 2015; Ivakhnenko et al., 2015*), mining exploration (*Farquharson and Craven, 2009; Abedi et al., 2013; Abdelrahman et al., 2016; Eshaghzadeh and Sahebari, 2020a; Eshaghzadeh et al., 2020*), engineering applications (*Dong et al., 2007*) geothermal activities (*Bektaş et al., 2007; Nyabeze and Gwavava, 2016*), archeological studies (*Gündoğdu et al., 2017*), and groundwater research (*Al-Garni, 2011; Araffa et al., 2015*).

Also, in the last two decades, general optimization methods have been used in many fields, as an alternative to these geophysical inversion methods (*Mehanee et al., 1998, Tarantola, 2005; Mehanee, 2022b*), such as genetic algorithm (*Boschetti et al., 1997; Kaftan, 2017*), particle swarm optimization (*van den Bergh and Engelbrecht, 2004; Essa and El-Hussein, 2017; Eshaghzadeh and Sahebari, 2020b; Eshaghzadeh and Hajian, 2021*), differential evolution or derivative (*Ekinci et al., 2016; Balkaya et al., 2017*), simulated annealing (*Biswas, 2015*), neural networks (*Al-Garni, 2013; Eshaghzadeh and Hajian, 2018; Eshaghzadeh et al., 2021*), ant colony optimization (*Colorni et al., 1991; Srivastava et al., 2014*), hybrid genetic price algorithm (*Bresco et al., 2005; Di Maio et al., 2016*) and teaching learning based optimization (*Eshaghzadeh and Hajian, 2020; Eshaghzadeh and Sahebari, 2020b*).

Automatic estimation of depth and shape of buried structure by magnetic data has attracted a lot of attention. Methods are generally divided into two categories. The first category is methods that can only be used for residual magnetic anomalies; Such as the methods presented by *Barbosa et al. (1999), Hsu (2002), Gerovska and Araúzo-Bravo (2003), Salem et al. (2004), Abdelrahman and Essa (2005), Abdelrahman et al. (2012)* and many others. However, the accuracy of the results obtained by these meth-

ods depends on the accuracy of the residual anomaly separated from the observational magnetic data.

The second category, on the other hand, not only can be used for the residual (local) magnetic field, but also can be used for observational (acquired) magnetic data. *Abdelrahman and Hassanein (2000)* presented a simple method for automatically determining the buried structure depth from magnetic data using a parametric relation. *Abdelrahman et al. (2007)* proposed a method of minimizing the least squares that the source depth is estimated using the second horizontal derivative of anomaly obtained from the magnetic data by applying filters of consecutive window lengths; They used the variance of the depths as a criterion for determining the correct shape and depth of the buried structure. However, the methods of *Abdelrahman and Hassanein (2000)* and *Abdelrahman et al. (2007)* can only be applied to magnetic data containing the combined effect of a residual field component of a complete local structure and a regional component presented with zero degrees and a first degree polynomial, respectively.

The PSO method was proposed by *Kennedy and Eberhart (1995)*. This method as well as its improved variations have been used more in the fields of artificial intelligence and computer. In recent years, the PSO particle swarm optimization method has been used in various branches of geophysics, and researchers have devised various methods to improve the performance of this algorithm (*Monteiro Santos, 2010; Toushmalani, 2013a and 2013b; Pallero et al., 2015; Singh and Biswas, 2016; Singh and Singh, 2017; Essa and El-Hussein, 2017; Roshan and Singh, 2017; Essa and Elhussein, 2018a, 2018b; Essa and Munschy, 2019, Eshaghzadeh and Sahebari, 2020b; Essa 2021; Eshaghzadeh and Hajian, 2021*).

2. Method

2.1. Forward modelling

According to *Abdelrahman and Essa (2015)*, the terms of horizontal, vertical, and total magnetic anomaly of spherical, horizontal cylinder, narrow plane, and geological contact models (Fig. 1) are defined as follows:

$$T(x_i, z) = K \frac{Az^2 + B(x_i - x_0) + C(x_i - x_0)^2}{((x_i - x_0)^2 + z^2)^q}, \tag{1}$$

where:

$$A = \begin{cases} 3\sin^2\theta - 1 \\ 2\sin\theta \\ -\cos\theta \\ \cos\theta \\ \cos\theta/z \end{cases} , \quad B = \begin{cases} -3z\sin 2\theta \\ -3z\cos\theta \\ -3z\sin\theta \\ 2z\sin\theta \\ \sin\theta \end{cases} ,$$

$$C = \begin{cases} 3\cos^2\theta - 1 & \text{for a sphere (total field)} \\ -\sin\theta & \text{for a sphere (vertical field)} \\ 2\cos\theta & \text{for a sphere (horizontal field)} \\ -\cos\theta & \text{for a horizontal cylinder, thin sheet (FHD), geological contact (SHD) (all fields)} \\ 0 & \text{for a thin sheet, geological contact (FHD) (all fields).} \end{cases}$$
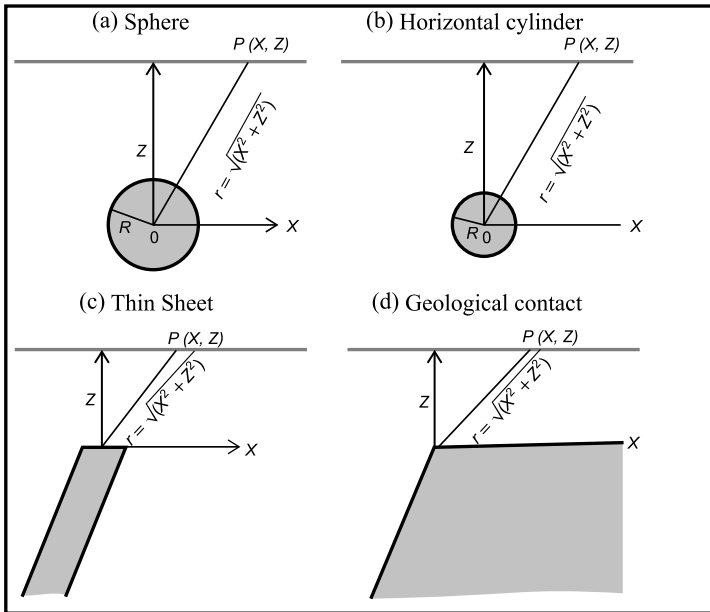

Fig. 1. Simple geometric structures.

In Equation (1), z is the depth of the centre of mass, x_i represents the coordinates of the data acquisition location, K is the amplitude coefficient, θ is the inclination angle parameter, and q is the shape factor. FHD and

SHD also refer to the second and first order of horizontal derivatives of magnetic anomalies, respectively. The shape factor for sphere, horizontal cylinder and narrow plate is 2.5, 2 and 1, respectively, which are equivalent to Euler's structural index of 3, 2 and 1, respectively. The definition of the inclination angle θ varies for different fields' components and sources (*Gay, 1963; Stanley, 1977; Prakasa Rao et al., 1986; Prakasa Rao and Subrahmanyam, 1988*).

2.2. Particle swarm optimization

The PSO algorithm is one of the evolved algorithms of artificial intelligence, based on collective intelligence, which is designed based on the evolutionary procedure of particles in a batch in order to achieve the optimal goal. In 1995, Eberhart and Kennedy first introduced PSO as an uncertain search method for functional optimization. This algorithm is inspired by the mass movement of birds looking for food. A group of birds randomly search for food in a space. There is only one piece of food in the space. None of the birds know the location of the food. One of the best strategies can be following the bird that has the shortest distance to the food. This strategy is actually the basis of the algorithm. Each solution (parameter) called a particle in the PSO algorithm is equivalent to a bird in the bird mass movement algorithm. Each particle has a merit value that is calculated by a merit function. The closer the particle is to the target in the search space (food in the bird movement model), the more suitable it is. Each particle also has a velocity that directs the particle's motion. Each particle continues to move in the space by following the optimal particles in the current state.

  In the standard PSO algorithm, each particle i (parameter under discussion) has two main parts, including the current position of the particle (x_i) (parameter value) and the current velocity of the particle (v_i) (the rate of changing the parameter value). The next position of each particle in the search space is determined by its current position and next velocity. The next velocity of each particle is determined by using the four main factors namely the current position of the particle, the current velocity of the particle, the best particle position ever experienced and stored in its memory (pbest) and the best position among the group particles which is called group experience (gbest). According to the above definitions, the next velocity of each particle (model parameter) i is expressed by the following

relation (*Sweilam et al., 2007*):

$$v_i(t+1) = W v_i(t) + c_1 \, \text{rand}(\text{pbest}(t) - x_i(t)) + c_2 \, \text{rand}(\text{gbest}(t) - x_i(t)). \,(2)$$

W is the weight factor of inertia that controls the effect of velocity in the previous step. c_1, c_2 are acceleration coefficients or individual and group learning coefficients of the particle. The rand command generates a random number in the range of zero to one. $v_i(t)$ is the i-th particle (parameter) velocity in the t-th iteration and $x_i(t)$ is the i-th particle value (parameter) in the t-th iteration. By determining the next velocity of each particle, its next position (parameter value) is obtained from the following equation:

$$x_i(t+1) = x_i(t) + v_i(t+1). \tag{3}$$

2.3. Improved global particle swarm optimization

In the improved global particle swarm optimization (IGPSO) algorithm to increase the convergence speed and minimize entrapment in local optimizations, we define the change rate of each parameter as follows:

$$v_{i,j}^{k+1} = A\left[1 + (r \times \delta)\right], \tag{4}$$

as

$$A = \left[w\, v_{i,j}^k + c_1 r_{1,j}^k \frac{\left(p_{i,\text{pbest}}^k - m_{i,j}^k\right)}{\text{rms}^{-1}} + c_2 r_{2,j}^k \frac{\left(p_{i,\text{gbest}}^k - m_{i,j}^k\right)}{\text{rms}} \right], \tag{5}$$

where 'rms' is the observational and computational magnetic error, $v_{i,j}^k$ is the velocity at k-th iteration, and $m_{i,j}^k$ is the position at k-th iteration. In the IGPSO algorithm, we also consider a high limit for the speed value $v_{i,j}^{k+1}$. If the value of A is more or less than the defined limits, the value of δ is considered equal to 1 and -1, respectively, otherwise the value of δ is assumed to be zero. r is a random number between 0 and 1.

Also in the proposed algorithm, we consider the acceleration coefficients dynamically, as:

$$c_1 = 2.5 - \frac{0.5\, t_{\text{iter}}}{T_{\text{max}}}, \tag{6}$$

$$c_2 = 1.5 + \frac{0.5\, t_{\text{iter}}}{T_{\text{max}}}\,, \tag{7}$$

t_{iter} is the current iteration and T_{max} is the maximum number of iterations. The value of $c_1 + c_2$ is always less than or equal to 4.

The inertia weight also changes as follows:

$$
\begin{aligned}
&w_{k+1} = (w_{\text{max}} - w_{\text{min}}) - (\text{rand}() - 0.5)\,2\,w_{\text{mean}} \\
&\text{if... } w_{k+1} < w_{\text{min}} \rightarrow w_{k+1} = w_{\text{min}} \\
&\text{if... } w_{k+1} > w_{\text{max}} \rightarrow w_{k+1} = w_{\text{max}}
\end{aligned}
\tag{8}
$$

Be careful that:

$$0 < w_{\text{max}}, w_{\text{min}} < 1\,,$$

w_{min} is the low weight limit, w_{max} is the high weight limit, w_{mean} is the average weight and rand() is a random number between 0 and 1.

As can be seen from the above equations, with the measures taken, c_1 decreases with increasing number of iterations. c_1 is pbest coefficient or the coefficient of the best position the particle has ever experienced. So the search is local, and as c_1 decreases, so does the local search. The coefficient rms^{-1} also improves the local search.

On the other hand, as the number of iterations increases, c_2 increases. c_2 is the coefficient of gbest or the best position of all the particles. So the search is done globally. Finally, as the number of iterations increases, the ability to search globally will increase and will help to find global optimization. For the third sentence, rms coefficient improves the global search.

Using the changes made in the PSO algorithm, it is possible to improve the PSO algorithm, and solve its problems and achieve the main answer which is universal (absolute) optimization.

The IGPSO operation algorithm is as follows:

1) The magnetic field data profile (artificial or real) is imported into the code written for the optimization algorithm based on the range defined for the certain number of unknown parameters of the model (geometric shape) that we consider. The statistical community (population) is made. Each member of the population has five components or parameters including of depth, amplitude coefficient, shape factor, magnetic inclination angle and origin coordinates.

2) Among the population, the member whose calculated magnetic field based on its parameters has the least error with the observational or theoretical magnetic field, is considered as the initial gbest.

3) In each iteration, by changing the speed, the value of the parameters of each member is improved and the best gbest is selected again among the improved population.

4) Finally, the condition for completing the algorithm can be considered as one of these two cases: a) the iteration continues until the defined number of iterations is completed. b) The iteration continues until the error between the computational and observational magnetic fields is less than the defined value.

It needs to be explained that the value of velocity in each iteration is actually a small numerical value (positive or negative) that is added or subtracted to the value obtained for the parameters in the previous iteration.

The IGPSO algorithm works repeatedly to optimize the unknown parameters of the model, and in each iteration the effect of the magnetic field in accordance with the parameters calculated for the model in that iteration, is calculated, then the amount of error between computational and observational magnetic data is estimated.

The error value between the calculated and observed magnetic data is obtained from the following relation (*Essa and Elhussein, 2018b*):

$$Q = \frac{2 \sum\limits_{i}^{N} |T_i^o - T_i^c|}{\sum\limits_{i}^{N} |T_i^o - T_i^c| + \sum\limits_{i}^{N} |T_i^o + T_i^c|} \, , \qquad (9)$$

where T_i^o is the observed magnetic field, and T_i^c is the computational magnetic field.

3. Numerical example

Figure 2 shows a horizontal magnetic field corresponding to an artificial spherical model located at a depth of 30 m whose center corresponds to the origin of the data profile (i.e. $x_0 = 0$). The magnetic inclination angle is 50 degrees and the amplitude coefficient is 10000 nT. m^3. The length of the magnetic data profile is 100 m, the data sampling distance is 1 m and the

magnitude of the magnetic field at the point of origin is -0.2381 nT. The assumed initial values for the parameters of this model are given in Table 1.

Although the origin point is specified and pre-defined in the numerical model, the *Stanley (1977)* method can also be used to determine the origin point. In this method, we connect the maximum and minimum amount of magnetic data in the direction of the profile (AB line in Fig. 2). The intersection point of this line with the change curve of the magnetic field can be considered as the origin of the profile.
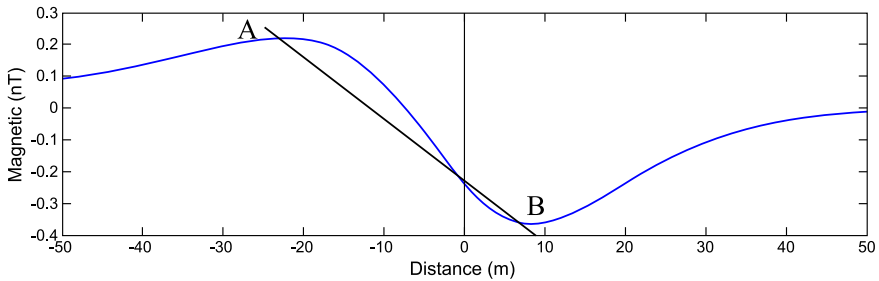

Fig. 2. The horizontal magnetic field corresponds to an artificial spherical model located at a depth of 30 m with a magnetic inclination angle of 50 degrees and an amplitude coefficient of 10000 nT. m^3, its centre corresponds to the origin of the data acquisition profile.

3.1. Modelling

For modelling with the improved IGPSO particle swarm optimization algorithm, one hundred initial models are produced according to the range considered for the parameters of depth, magnetic inclination angle, amplitude coefficient, origin point coordinates and shape factor (Table 1). In each iteration, the value of the parameters is changed and the magnetic field is calculated for the new variables, and the error between the calculated and observational magnetic field is determined. In each iteration, the program checks that the value of the calculated parameters does not exceed the maximum or minimum values defined in Table 1. The minimum error to stop repetition based on the objective function (Eq. (9)) is 0.01. The intended number of repetitions for each program execution is 80 repetitions, in which the final values obtained for each parameter are stored. The code for the improved IGPSO particle swarm optimization algorithm is written in MAT-LAB, and it runs for 30 independent iterations. So at the end of the code

Table 1. The considered range for the artificial model parameters and the results obtained from the IGPSO algorithm.

Parameters		Z (m)	K (nT.m^3)	θ (deg)	X_0 (m)	q	Q
Initial values		30	10000	50	0	2.5	–
Used ranges		25 to 35	8000 to 12000	45 to 55	−5 to 5	0/5 to 30	–
Computed values	Without noise	31	10500/8	49/36	−0/515	2.44	0/0442
	With noise	30/56	9666/8	50/32	−1/19	2.44	0/1055

execution, there will be 30 calculated values for each variable. Frequency charts are drawn for each parameter and the average of the range with the highest answer will be considered as the final value of that parameter.

Figures 3a to 3e show the frequency charts corresponding to the values obtained for the depth parameters, amplitude coefficient, origin point coordinates, inclination angle, and shape factor. According to the recent figures, the maximum values calculated for the parameters of depth, amplitude coefficient, origin point coordinates, inclination angle, and shape factor are in the ranges of 30.5 to 31.5 m, 10200 to 10600 nT.m^3, −0.25 up to −0.75 m, 48.5 to 49.5 degrees and 2.3 to 2.5, respectively.

Based on the averaging method, for the parameters of depth, amplitude coefficient, coordinates of the origin point, inclination angle, and shape factor, the following values are obtained, respectively: 31 m, 10500.8 nT.m^3, 49.36 degrees, −0.515 m and 2.44. (Table 1). Figure 4a shows the theoretical magnetic field as well as the magnetic field generated using the global particle swarm optimization method, and Figure 4b shows the difference between the theoretical magnetic field and the magnetic field calculated at the corresponding measurement points. The error obtained between the theoretical magnetic field and the calculated magnetic field, based on the values obtained for the model parameters is 0.0442.

To evaluate the efficiency of the improved particle swarm optimization algorithm in the presence of noise, a random noise was added to the theoretical magnetic field based on the following equation (*Abdelrahman and Essa, 2015*):

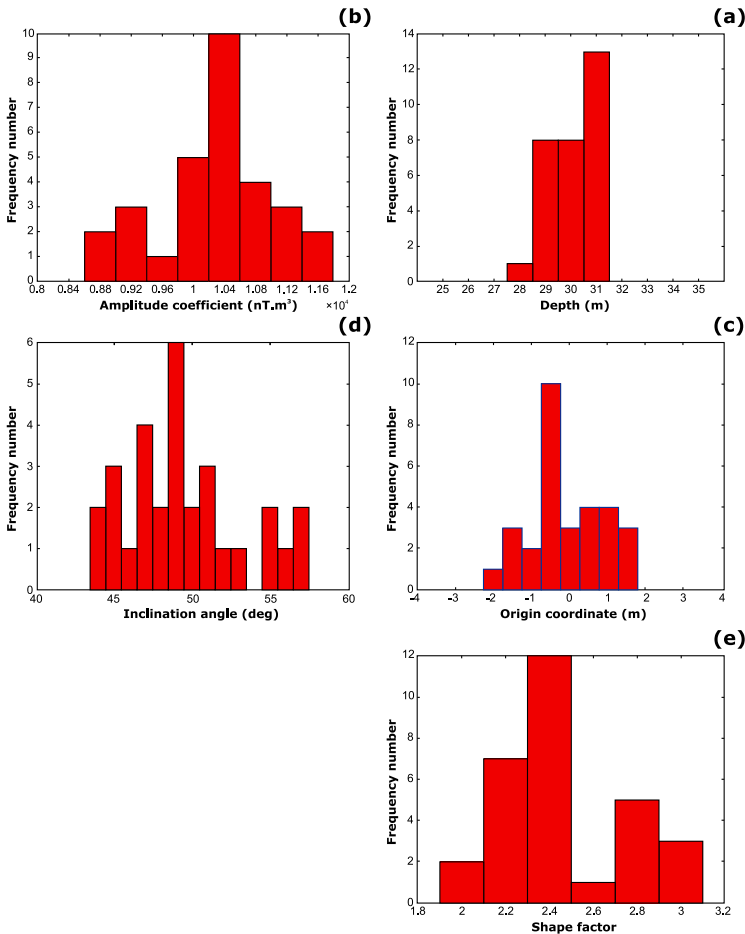$$T_{\text{noise}}(x_i) = T(x_i) + K \left(\text{rand}(i) - 0.5 \right). \tag{10}$$

Fig. 3. Frequency chart corresponding to the values obtained for the parameters a) depth, b) amplitude coefficient, c) origin point coordinates, d) inclination angle, and e) shape factor using the improved global particle swarm optimization algorithm for theoretical magnetic noiseless data.

In the latter equation, $T_{\text{noise}}(x_i)$ is the noisy magnetic field at a point x_i, k is a constant number that determines the amplitude and magnitude of the noise (which is 0.05 for this model), that depends on the magnitude of the magnetic field amplitude, and rand is a random number between 0 and 1.

The frequency charts corresponding to the values obtained from the analysis of noisy magnetic data for the parameters of depth, amplitude
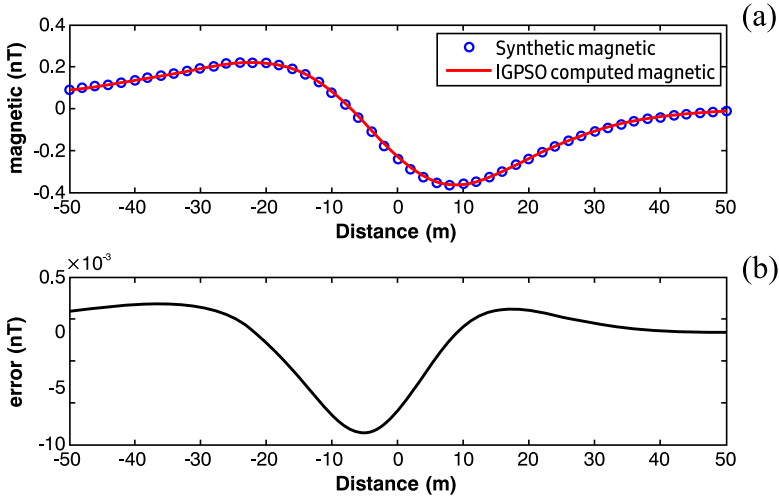
Fig. 4. a) Theoretical magnetic field and also the magnetic field obtained by the improved global particle swarm optimization method, b) The difference between the theoretical magnetic field and the magnetic field calculated at the corresponding measuring points.

coefficient, origin point coordinates, inclination angle and shape factor are shown in Figure 5a to Figure 5e. According to the recent figures, the maximum values calculated for the parameters of depth, amplitude coefficient, origin point coordinates, inclination angle and shape factor, respectively, are in the ranges of 29.5 to 30.5 m, 9400 to 9800 nT. m^3, −0.75 to −1.25 m, 50.5 to 51.5 degrees and 2.3 to 2.5.

Based on the averaging method, the following values are obtained for the parameters of depth, amplitude coefficient, origin point coordinates, inclination angle and shape factor, respectively: 30.56 m, 9666.8 nT. m^3, −1.19 m, 51.32 degrees, and 2.44 (Table 1). Figure 6a shows the theoretical noisy magnetic field, as well as the magnetic field obtained by using the improved global particle swarm optimization method, and Figure 6b shows the difference between the theoretical noisy magnetic field and the magnetic field calculated at the corresponding measuring points. The error between the theoretical noisy magnetic field and the calculated magnetic field is 0.1055, based on the values obtained for the model parameters.

According to Table 1, the error between the initial values and the calculated values for the parameters of depth, amplitude coefficient, origin point coordinates, inclination angle and shape factor for non-noise magnetic field
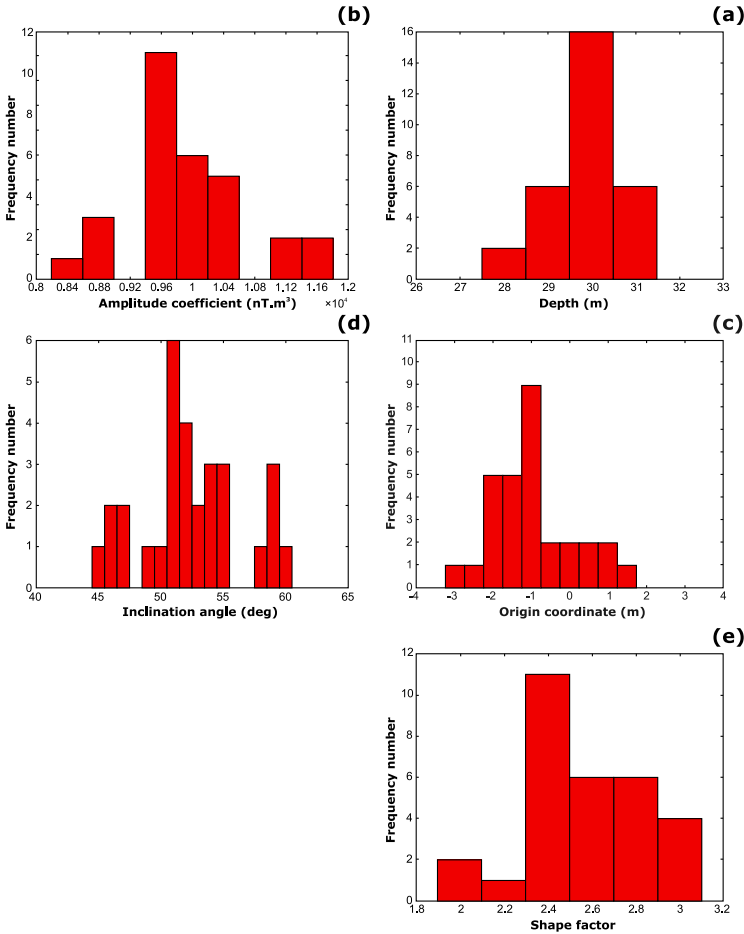
Fig. 5. Frequency diagram corresponding to the values obtained for the parameters a) depth, b) amplitude coefficient, c) origin point coordinates, d) inclination angle and e) shape factor using the improved global particle swarm optimization algorithm for the theoretical noisy magnetic data.

are 1 m, 500.8 nT. m^3, -0.515 m, 0.64 degrees and 0.06, respectively, and for the noisy magnetic field are 0.56 m, 333.2 nT. m^3, -1.19 m, 0.32 degrees and 0.06, respectively. Based on the results of theoretical magnetic field inversion, without noise and with noise, the improved global particle swarm optimization algorithm can be considered as an effective method with acceptable performance for the analysis of the magnetic fields.
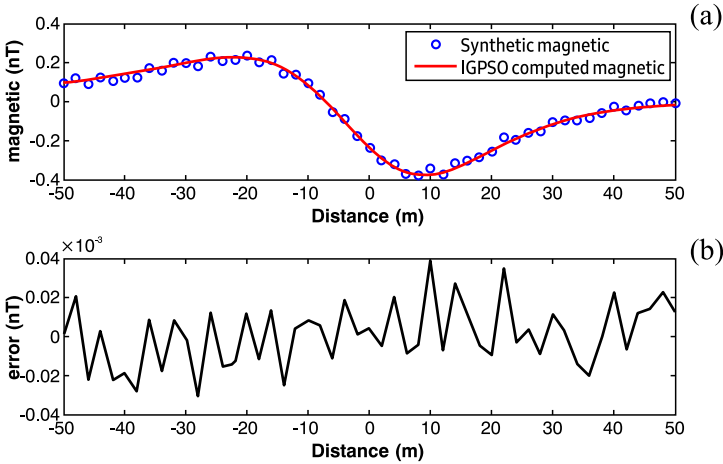
Fig. 6. a) Theoretical noisy magnetic field and also the magnetic field obtained by the improved global particle swarm optimization method, b) The difference between the theoretical noisy magnetic field and the calculated magnetic field at the corresponding measuring points.

4. Field example

4.1. Geographical location and geology of Ileh region in Iran

In terms of geographical location, the study area is located in Khorasan Razavi province, Taibad city and a village called Ileh, which is significant in terms of iron reserves. Magnetometric measurements of the study area are located in the geological map of 1/250000 Taibad.

The main outcrop of geological units in this area is the undivided volcanic-sedimentary unit, which is mainly tuff-Chile. The age of this unit is Late Proterozoic, which has undergone a distinct regional metamorphism, and this unit has a northeast-southwest trend and a light colour (Fig. 7).

4.2. Ileh region magnetic field

The acquisition of magnetic data in the Ileh region was done simultaneously with three devices and one device in the region as a base station for daily correction of data. In this area, the distances between profiles were 50 m in the north-south direction and the distance of the stations was 20 m, and in some areas 10 m. The area is 688900 m^2 with dimensions of 830×830 m,
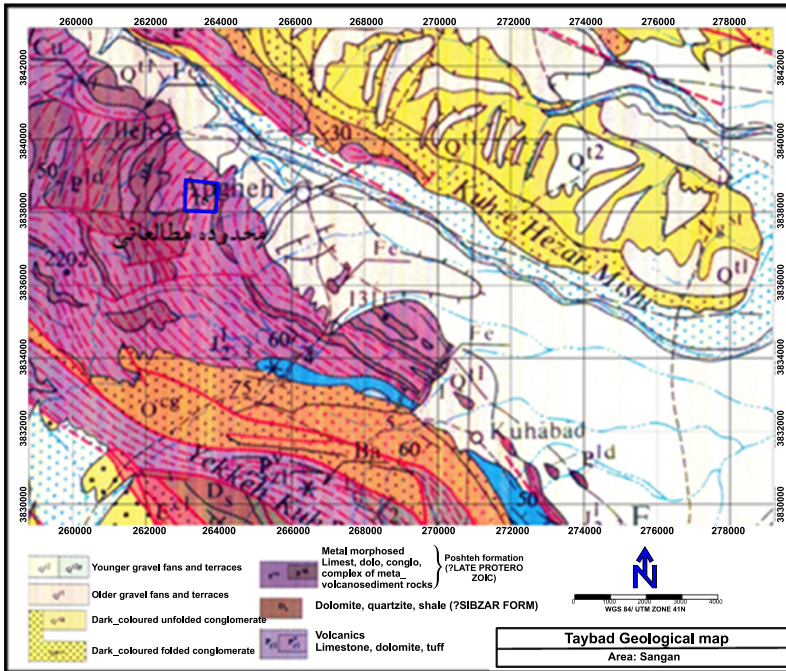
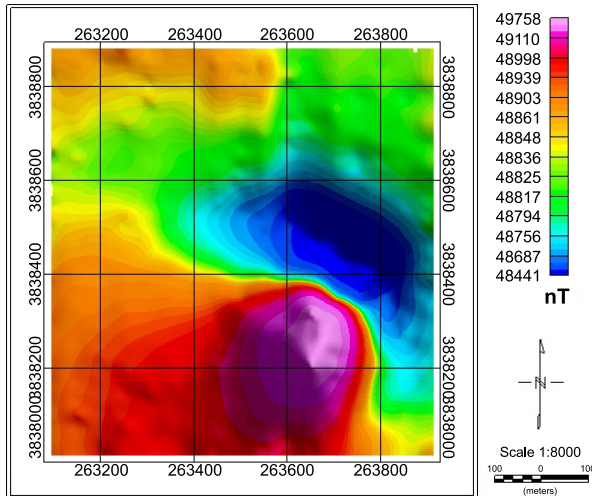Fig. 7. Geological map of the study area (Ileh).

Fig. 8. Magnetic field of the study area in Ile region.

295

in which a total of 17 profiles and 589 points of magnetic field data are acquired in this area.

Figure 8 shows the magnetic field of the study area. A bipolar magnetic anomaly with a maximum of 49758 nT and a minimum of 48441 nT is observed, in the south-eastern part of the study area.

The magnetic field in Figure 8 also contains magnetic fields from regional and local structures in the study area. Therefore, it is necessary to remove the effect of the regional magnetic field from the residual magnetic field data obtained after IGRF correction (declination and inclination angle values and IGRF are 3.5, 53.3 and 49194, respectively), in order to finally obtain the desired local magnetic field map. If there is no dominant regional field in the data collection area, the local field obtained from the surface trend filter will not differ from the field obtained from the IGRF correction.

Figure 9 shows the residual (local) magnetic field of the study area for the first-order surface trend. After removing the effect of the regional magnetic field, the maximum and minimum values of the magnetic field change. The local magnetic field map is suitable for quantitative analysis, as it shows exactly the values of the magnetic field of the magnetic source in the study area.
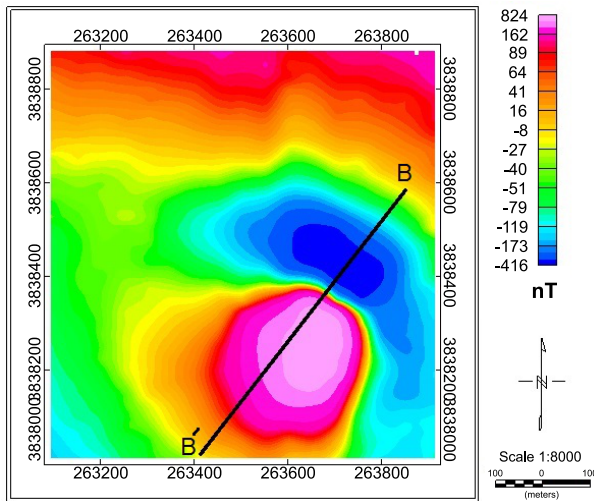

Fig. 9. Position and direction of BB' profiles on magnetic anomalies in the local magnetic field map of Ileh region.

4.3. Inversion results

To model the source of the magnetic anomaly with the improved global particle swarm optimization method, the BB′ profile with a length of 710 m is designed according to Fig. 9, on the effect of the magnetic field of the anomaly source in Geosoft software. Data collection was performed at 72 points with a distance of 10 m. Figure 10 shows the changes in the magnetic field along the BB′ profile. As mentioned in the Numerical example section, One method to determine the point of origin is to use the Stanley method (*Stanley, 1977*), which is very efficient for real magnetic field profiles. In this method, we connect the maximum and minimum amount of magnetic data in the direction of the profile. The point of contact of this curve with the change curve of the magnetic field can be considered as the origin of the profile. The method presented is particularly simple to execute, does not require computing facilities, and does not depend upon skilled subjective judgments. In BB′ profile, the coordinates of the origin point is 310 m (in Fig. 10, the point of intersection of the EF line that connects the minimum and maximum amount of magnetic field in the direction of the BB′ profile with the curve of magnetic field changes).
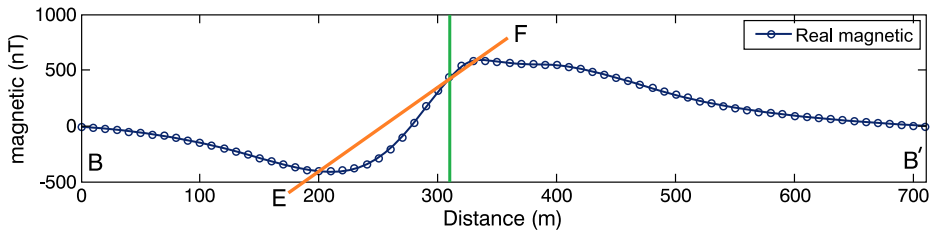

Fig. 10. Changes in the magnetic field in the direction of the BB′ profile.

For modelling with improved particle swarm optimization (IGPSO) algorithm method, one hundred and twenty initial models is produced according to the considered range for structural parameters of depth, amplitude coefficient, origin point coordinates, inclination angle and shape factor selected based on geological information (Table 2). As mentioned before, the program checks in each iteration that the value of the calculated parameters does not exceed the maximum and minimum values defined in Table 2. The minimum error considered to stop iteration is 0.1, based on the objective function (Eq. (9)).

Table 2. Considered range and obtained values from the magnetic field analysis of Ileh region (interpretation results).

Parameters	Z (m)	K (nT. m^3)	θ (deg)	X (m)	q	Q
Initial values	70 to 140	100000 to 400000	30 to 80	200 to 400	0/5 to 3	–
Used ranges	112/5 to 117/5	195000 to 205000	57/5 to 62/5	315 to 325	1/7 to 1/8	–
Computed values	114/9	201450	60/2	316/4	1/76 (∼Cylinder)	26/0

The intended number of repetitions for each program execution is 20 repetitions, in which the final obtained values of each parameter are stored. To analyse the magnetic field of Faryab region, the code written in MATLAB for improved particle swarm optimization (IGPSO) algorithm runs for 50 independent iterations. So at the end of the code execution, there will be 50 calculated values for each variable. Similar to the artificial models, frequency graphs are plotted for each parameter and the average of the values of the range in which the most answers are located is considered as the final value of that parameter.

The frequency diagram corresponding to the values obtained for the parameters of depth, amplitude coefficient, coordinates of the starting point, inclination angle and shape factor is shown in Figs. 11a to 11e.

According to Figure 11, the maximum values calculated for the parameters of depth, amplitude coefficient, origin point coordinates, inclination angle and shape factor are in the ranges of 112.5 to 117.5 m, 195000 to 205000 nT. m^3, 315 to 325 m, 57.5 to 62.5 degrees, and 1.7 to 1.8, respectively. As mentioned before, the average values in these ranges are considered as the final values for the parameters of the buried structure, which are 114.9 m, 201450 nT. m^3, 316.4 m, 60.2 degrees, and 1.76 for the parameters of depth, amplitude coefficient, coordinates of the origin point, inclination angle, and shape factor, respectively (Table 2).

Figure 12a shows the measured (observational) magnetic field as well as the calculated magnetic field using the improved IGPSO particle swarm optimization method. Figure 12b shows the difference between the observed magnetic field and the calculated magnetic field at corresponding measuring points. The error between the observed magnetic field and the calculated

magnetic field is 0.26, based on the values obtained for the structural parameters.

Based on the estimated shape factor value, the shape of the subsurface mass is geometrically closer to the horizontal cylinder. Also, the value of the origin coordinates obtained by the improved global particle swarm optimization method is 316.5 m, which is an acceptable accordance with the value obtained by the *Stanley (1977)* method, i.e. 310 m.
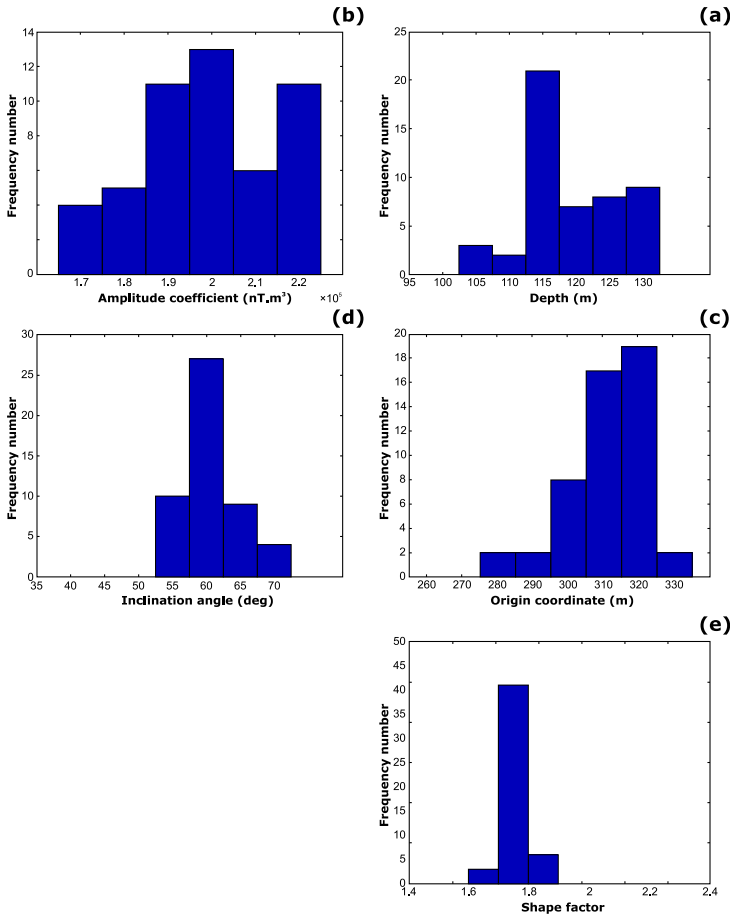

Fig. 11. Frequency diagram corresponding to the values obtained for the parameters a) depth, b) amplitude coefficient, c) origin point coordinates, d) inclination angle and e) shape factor using the improved global particle swarm optimization algorithm for magnetic data of the study area in Ileh.
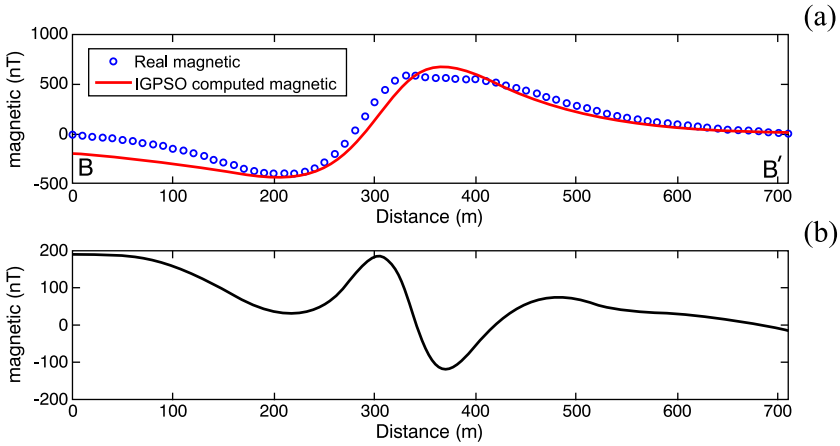
Fig. 12. a) The measured magnetic field and the calculated magnetic field using the improved global particle swarm optimization method. b) The difference between the observed magnetic field and the calculated magnetic field at the corresponding measuring points.

5. Conclusion

In this paper, an improved global particle swarm optimization algorithm which is based on the initial population definition is used for inverse modelling of magnetic data. This method is capable of analysing the magnetic field data that have not been transferred to the pole or equator with acceptable accuracy, provided that the values of the subsurface structure parameters are within the assumed initial numerical range for the model parameters.

The results obtained from the numerical example show that the improved global particle swarm optimization method is able to estimate the model parameters with acceptable accuracy. Due to the good performance of this method (with and without random noise), we used it for modelling a two-dimensional magnetic field in Ileh village.

There is a good accordance between the magnetic field calculated based on the parameters estimated using the improved global particle swarm optimization algorithm and the trend of changes in the magnetic field measured in the direction of the data acquisition profile, so that the error is 0.26. The estimated depth by the improved global particle swarm optimization

300

algorithm for the centre of the mass is 114.9 m, which is an acceptable accordance with the average depth obtained for the centre of the buried mass using drilling which is 103.2 m.

References

Abdelrahman E. M., Abo-Ezz E. R., Essa K. S., 2012: Parametric inversion of residual magnetic anomalies due to simple geometric bodies. Explor. Geophys., **43**, 3, 178–189, doi: 10.1071/EG11026.

Abdelrahman E. M., Abo-Ezz E. R., Essa K. S., El-Araby T. M., Soliman K. S., 2007: A new least-squares minimization approach to depth and shape determination from magnetic data. Geophys. Prospect., **55**, 3, 433–446, doi: 10.1111/j.1365-2478.2007.00621.x.

Abdelrahman E. M., Essa K. S., 2005: Magnetic interpretation using a least-squares, depth-shape curves methods. Geophysics, **70**, 3, L23–L30, doi: 10.1190/1.1926575.

Abdelrahman E. M., Essa K. S., 2015: A new method for depth and shape determinations from magnetic data. Pure Appl. Geophys., **172**, 2, 439–460, doi: 10.1007/s00024-014-0885-9.

Abdelrahman E. M., Essa K. S., El-Araby T. M., Abo-Ezz E. R., 2016: Depth and shape solutions from second moving average residual magnetic anomalies. Explor. Geophys., **47**, 1, 58–66, doi: 10.1071/EG14073.

Abdelrahman E. M., Hassanein H. I., 2000: Shape and depth solutions from magnetic data using a parameteric relationship. Geophysics, **65**, 1, 126–131, doi: 10.1190/1.1444703.

Abdelrahman E. M., Soliman K. S., Abo-Ezz E. R., El-Araby T. M., Essa K. S., 2009: A least-squares standard deviation method to interpret magnetic anomalies due to thin dikes. Near Surf. Geophys., **7**, 1, 41–46, doi: 10.3997/1873-0604.2008032.

Abedi M., Gholami A., Norouzi G.-H., 2013: A stable downward continuation of airborne magnetic data: A case study for mineral prospectivity mapping in Central Iran. Comput. Geosci., **52**, 269–280, doi: 10.1016/j.cageo.2012.11.006.

Abubakar R., Muxworthy A. R., Sephton M. A., Southern P., Watson J. S., Fraser A. J., Almeida T. P., 2015: Formation of magnetic minerals at hydrocarbon-generation conditions. Mar. Pet. Geol., **68**, Part A, 509–519, doi: 10.1016/j.marpetgeo.2015.10.003.

Al-Garni M. A., 2011: Magnetic and DC resistivity investigation for groundwater in a complex subsurface terrain. Arab. J. Geosci., **4**, 3-4, 385–400, doi: 10.1007/s12517-009-0071-z.

Al-Garni M. A., 2013: Inversion of residual gravity anomalies using neural network. Arab. J. Geosci., **6**, 5, 1509–1516, doi: 10.1007/s12517-011-0452-y.

Araffa S. A. S., Helaly A. S., Khozium A., Lala A. M. S., Soliman S. A., Hassan N. M., 2015: Delineating groundwater and subsurface structures by using 2D resistivity, gravity and 3D magnetic data interpretation around Cairo–Belbies Desert road,

Egypt. NRIAG J. Astron. Geophys., **4**, 1, 134–146, `doi: 10.1016/j.nrjag.2015.06.004`.

Balkaya C., Ekinci Y. L., Göktürkler G., Turan S., 2017: 3D non-linear inversion of magnetic anomalies caused by prismatic bodies using differential evolution algorithm. J. Appl. Geophys., **136**, 372–386, `doi: 10.1016/j.jappgeo.2016.10.040`.

Barbosa V. C. F., Silva J. B. C., Medeiros W. E., 1999: Stability analysis and improvement of structural index estimation in Euler deconvolution. Geophysics, **64**, 1, 48–60, `doi: 10.1190/1.1444529`.

Bektaş Ö., Ravat D., Büyüksaraç A., Bilim F., Ateş A., 2007: Regional geothermal characterisation of East Anatolia from aeromagnetic, heat flow and gravity data. Pure Appl. Geophys., **164**, 5, 975–998, `doi: 10.1007/s00024-007-0196-5`.

Biswas A., 2015: Interpretation of residual gravity anomaly caused by a simple shaped body using very fast simulated annealing global optimization. Geosci. Front., **6**, 6, 875–893, `doi: 10.1016/j.gsf.2015.03.001`.

Biswas A., Rao K., 2021: Interpretation of magnetic anomalies over 2D fault and sheet-type mineralized structures using very fast simulated annealing global optimization: An understanding of uncertainty and geological implications. Lithosphere, **2021**, Special 6, 2964057, `doi: 10.2113/2021/2964057`.

Boschetti F., Dentith M. C., List R. D., 1997: Inversion of potential field data by genetic algorithms. Geophys. Prospect., **45**, 3, 461–478, `doi: 10.1046/j.1365-2478.1997.3430267.x`.

Bresco M., Raiconi G., Barone F., De Rosa R., Milano L., 2005: Genetic approach helps to speed classical Price algorithm for global optimization. Soft Comput., **9**, 7, 525–535, `doi: 10.1007/s00500-004-0370-y`.

Colorni A., Dorigo M., Maniezzo V., 1991: Distributed optimization by ant colonies. In: Varela F., Bourgine P. (Eds.): Proceedings of the 1st European Conference on Artificial Life, ECAL'91, Paris, Elsevier Publishing, Amsterdam, 134–142.

Di Maio R., Rani P., Piegari E., Milano L., 2016: Self-potential data inversion through a Genetic-Price algorithm. Comput. Geosci., **94**, 86–95, `doi: 10.1016/j.cageo.2016.06.005`.

Dong P., Fan J.-L., Liu Z.-H., Chen G.-W., Wang L.-S., Sun B., Pu X.-X., 2007: Magnetic anomaly characteristics out of reinforcement cage in cast-in situ pile. Prog. Geophys., **22**, 5, 1660–1665 (in Chinese).

Ekinci Y. L., Balkaya Ç., Şeren A., Kaya M. A., Lightfoot C. S., 2014: Geomagnetic and geoelectrical prospection for buried archaeological remains on the Upper City of Amorium, a Byzantine City in midwestern Turkey. J. Geophys. Eng., **11**, 1, 015012, `doi: 10.1088/1742-2132/11/1/015012`.

Ekinci Y. L., Balkaya Ç., Göktürkler G., Turan S., 2016: Model parameter estimations from residual gravity anomalies due to simple-shaped sources using Differential Evolution Algorithm. J. Appl. Geophys., **129**, 133–147, `doi: 10.1016/j.jappgeo.2016.03.040`.

Eshaghzadeh A., Hajian A., 2018: 2D inverse modeling of residual gravity anomalies from simple geometric shapes using Modular Feed-forward Neural Network. Ann. Geophys., **61**, 1, SE115, `doi: 10.4401/ag-7540`.

302

Eshaghzadeh A., Hajian A., 2020: Multivariable modified teaching learning based optimization (MM-TLBO) algorithm for inverse modeling of residual gravity anomaly generated by simple geometric shapes. J. Environ. Eng. Geophys., **25**, 4, 463–476, `doi: 10.32389/JEEG20-003`.

Eshaghzadeh A., Hajian A., 2021: 2-D gravity inverse modelling of anticlinal structure using improved particle swarm optimization (IPSO). Arab. J. Geosci., **14**, 14, 1378, `doi: 10.1007/s12517-021-07798-6`.

Eshaghzadeh A., Sahebari S. S., 2020a: Multivariable teaching-learning-based optimization (MTLBO) algorithm for estimating the structural parameters of the buried mass by magnetic data. Geofizika, **37**, 2, 213–235, `doi: 10.15233/gfz.2020.37.6`.

Eshaghzadeh A., Sahebari S. S., 2020b: Application of PSO Algorithm based on the mean value of maximum frequency distribution for 2-D inverse modeling of gravity data due to a finite vertical cylinder shape. Quad. di Geofis., **162**, 1–22, `doi: 10.13127/qdg/162`.

Eshaghzadeh A., Sahebari S. S., Kalantari R. A., 2020: Determination of sheet-like geological structures parameters using Marquardt inversion of the magnetic data. Indian J. Geo-Mar. Sci., **49**, 3, 450–457.

Eshaghzadeh A., Sahebari S. S., Kalantari R. A., 2021: 2-D anticlinal structure modeling using feed-forward neural network (FNN) inversion of profile gravity data: A case study from Iran. J. Earth Space Phys., **46**, 4, 79–91, `doi: 10.22059/jesphys.2021.286888.1007148`.

Essa K. S., 2021: Evaluation of the parameters of fault-like geologic structure from the gravity anomalies applying the particle swarm. Environ. Earth Sci., **80**, 15, 489, `doi: 10.1007/s12665-021-09786-1`.

Essa K. S., El-Hussein M., 2017: 2D dipping dike magnetic data interpretation using a robust particle swarm optimization. Geosci. Instrum. Methods Data Syst. Discuss., `doi: 10.5194/gi-2017-39`.

Essa K. S, Elhussein M., 2018a: Gravity data interpretation using different new algorithms: A comparative study. In: Zouaghi T. (Ed.): Gravity – Geoscience Applications, Industrial Technology and Quantum Aspect, Licensee InTech., `doi: 10.5772/intechopen.71086`.

Essa K. S., Elhussein M., 2018b: PSO (particle swarm optimization) for interpretation of magnetic anomalies caused by simple geometrical structures. Pure Appl. Geophys., **175**, 10, 3539–3553, `doi: 10.1007/s00024-018-1867-0`.

Essa K. S., Mehanee S., Elhussein M., 2021: Magnetic data profiles interpretation for mineralized buried structures identification applying the variance analysis method. Pure Appl. Geophys., **178**, 3, 973–993, `doi: 10.1007/s00024-020-02553-6`.

Essa K. S., Munschy M., 2019: Gravity data interpretation using the particle swarm optimization method with application to mineral exploration. J. Earth Syst. Sci., **128**, 5, 123, `doi: 10.1007/s12040-019-1143-4`.

Farquharson C. G., Craven J. A., 2009: Three-dimensional inversion of magnetotelluric data for mineral exploration: An example from the McArthur River uranium deposit, Saskatchewan, Canada. J. Appl. Geophys., **68**, 4, 450–458, `doi: 10.1016/j.jappgeo.2008.02.002`.

Gan J., Li H., He Z., Gan Y., Mu J., Liu H., Wang L., 2022: Application and significance of geological, geochemical, and geophysical methods in the Nanpo gold field in Laos. Minerals, **12**, 96, doi: 10.3390/min12010096.

Gay S. P., 1963: Standard curves for interpretation of magnetic anomalies over long tabular bodies. Geophysics, **28**, 2, 161–200, doi: 10.1190/1.1439164.

Gerovska D., Araúzo-Bravo M. J., 2003: Automatic interpretation of magnetic data based on Euler deconvolution with unprescribed structural index. Comput. Geosci., **29**, 8, 949–960, doi: 10.1016/S0098-3004(03)00101-8.

Gokula A. P., Sastry R. G., 2022: Total magnetic-field intensity anomaly due to a vertical pyramid model of flat top and bottom with constant magnetisation. J. Earth Syst. Sci., **131**, 1, 8, doi: 10.1007/s12040-021-01758-0.

Gündoğdu N. Y., Candansayar M. E., Genç E., 2017: Rescue archaeology application: Investigation of Kuriki Mound archaeological area (Batman, SE Turkey) by using direct current resistivity and magnetic methods. J. Environ. Eng. Geophys., **22**, 2, 177–189, doi: 10.2113/JEEG22.2.177.

Hsu S.-K., 2002: Imaging magnetic sources using Euler's equation. Geophys. Prospect., **50**, 1, 15–25, doi: 10.1046/j.1365-2478.2001.00282.x.

Ivakhnenko O. P., Abirov R., Logvinenko A., 2015: New method for characterisation of petroleum reservoir fluidmineral deposits using magnetic analysis. Energy Procedia, **76**, 454–462, doi: 10.1016/j.egypro.2015.07.877.

Kaftan İ., 2017: Interpretation of magnetic anomalies using a genetic algorithm. Acta Geophys., **65**, 4, 627–634, doi: 10.1007/s11600-017-0060-7.

Kennedy J., Eberhart R., 1995: Particle swarm optimization. Proceedings of the IEEE International Conference on Neural Networks, 4, 1942–1948, doi: 10.1109/ICNN.1995.488968.

Mehanee S., 2022a: A new scheme for gravity data interpretation by a faulted2-D horizontal thin block: Theory, numerical examples and real data investigation. IEEE Trans. Geosci. Remote Sens., **60**, 4705514, 1–14, doi: 10.1109/TGRS.2022.3142628.

Mehanee S., 2022b: Simultaneous joint inversion of residual gravity and self-potential data measured along profile: Theory, numerical examples and a case study from mineral exploration with cross validation from electromagnetic data. IEEE Trans. Geosci. Remote Sens., **60**, 4701620, 1–20, doi: 10.1109/TGRS.2021.3071973.

Mehanee S., Essa K. S., Diab Z. E., 2021: Magnetic data interpretation using a new R-parameter imaging method with application to mineral exploration. Nat. Resour. Res., **30**, 1, 77–95, doi: 10.1007/s11053-020-09690-8.

Mehanee S., Golubev N., Zhdanov M. S., 1998: Weighted regularized inversion of magnetotelluric data. SEG Technical Program Expanded Abstracts 1998, presented at the 68th International and Meeting, Society of Exploration Geophysicists, New Orleans, Louisiana, USA, doi: 10.1190/1.1820468.

Monteiro Santos F. A., 2010: Inversion of self-potential of idealized bodies' anomalies using particle swarm optimization. Comput. Geosci., **36**, 9, 1185–1190, doi: 10.1016/j.cageo.2010.01.011.

Nabighian M. N., Grauch V. J. S., Hansen R. O., LaFehr T. R., Li Y., Peirce J. W., Phillips J. D., Ruder M. E., 2005: The historical development of the magnetic method in exploration. Geophysics, **70**, 6, 33ND–61ND, `doi: 10.1190/1.2133784`.

Nyabeze P. K., Gwavava O., 2016: Investigating heat and magnetic source depths in the Soutpansberg Basin, South Africa: Exploring the Soutpansberg Basin Geothermal Field. Geotherm. Energy, **4**, 8, `doi: 10.1186/s40517-016-0050-z`.

Pallero J. L. G., Fernández-Martínez J. L., Bonvalot S., Fudym O., 2015: Gravity inversion and uncertainty assessment of basement relief via Particle Swarm Optimization. J. Appl. Geophys., **116**, 180–191, `doi: 10.1016/j.jappgeo.2015.03.008`.

Prakasa Rao T. K. S., Subrahmanyam M., Srikrishna Murthy A., 1986: Nomograms for the direct interpretation of magnetic anomalies due to long horizontal cylinders. Geophysics, **51**, 11, 2156–2159, `doi: 10.1190/1.1442067`.

Prakasa Rao T. K. S., Subrahmanyam M., 1988: Characteristic curves for inversion of magnetic anomalies of spherical ore bodies: Pure Appl. Geophys., **126**, 1, 69–83, `doi: 10.1007/BF00876915`.

Roshan R., Singh U. K., 2017: Inversion of residual gravity anomalies using tuned PSO. Geosci. Instrum. Methods Data Syst., **6**, 1, 71–79, `doi: 10.5194/gi-6-71-2017`.

Salem A., Ravat D., Mushayandebvu M. F., Ushijima K., 2004: Linearized least-squares method for interpretation of potential field data from sources of simple geometry. Geophysics, **69**, 3, 783–788, `doi: 10.1190/1.1759464`.

Singh A., Biswas A., 2016: Application of global particle swarm optimization for inversion of residual gravity anomalies over geological bodies with idealized geometries. Nat. Resour. Res., **25**, 3, 297–314, `doi: 10.1007/s11053-015-9285-9`.

Singh K. K., Singh U. K., 2017: Application of particle swarm optimization for gravity inversion of 2.5-D sedimentary basins using variable density contrast. Geosci. Instrum. Methods Data Syst., **6**, 1, 193–198, `doi: 10.5194/gi-6-193-2017`.

Srivastava S., Datta D., Agarwal B. N. P., Mehta S., 2014: Applications of ant colony optimization in determination of source parameters from total gradient of potential fields. Near Surf. Geophys., **12**, 3, 373–389, `doi: 10.1002/nsg.123001`.

Stanley J. M., 1977: Simplified magnetic interpretation of the geologic contact and thin dike. Geophysics, **42**, 6, 1236–1240, `doi: 10.1190/1.1440788`.

Sweilam N. H., El-Metwally K., Abdelazeem M., 2007: Self potential signal inversion to simple polarized bodies using the particle swarm optimization method: A visibility study. Egypt. J. Appl. Geophys., **6**, 1, 195–208.

Tarantola A., 2005: Inverse problem theory and methods for model parameters estimation. The Society for Industrial and Applied Mathematics, 339 p.

Toushmalani R., 2013a: Comparison result of inversion of gravity data of a fault by particle swarm optimization and Levenberg-Marquardt methods. SpringerPlus, **2**, 462, `doi: 10.1186/2193-1801-2-462`.

Toushmalani R., 2013b: Gravity inversion of a fault by Particle Swarm Optimization (PSO). SpringerPlus, **2**, 315, `doi: 10.1186/2193-1801-2-315`.

van den Bergh F., Engelbrecht A. P., 2004: A cooperative approach to particle swarm optimization. IEEE Trans. Evol. Comput., **8**, 3, 225–239, `doi: 10.1109/TEVC.2004.826069`.